LIQUIDUS EQUILIBRIA OF LUNAR ANALOGS AT HIGH PRESSURE.

J. Longhi, Lamont-Doherty Earth Observatory, Palisades, NY 10964

Melting experiments have been performed in the range of 20 to 40 kbar on partially crystallized synthetic glasses in order to test the accuracy of the polybaric fractional fusion model for picritic lunar green glasses (1). Results show that the model predicts the position of the olivine(ol) + orthopyroxene(opx) liquidus boundary within the uncertainty of the measurements, but that details of the calculations are subject to change because of new crystal/liquid partitioning data for olivine and pyroxene.

Volcanic glasses with picritic compositions (2) have posed a thorny problem for petrologists: their compositions are multiply-saturated with olivine and orthopyroxene at pressures of 17.5 to 25 kbar (cf. 3) and traditionally the pressure of multiple saturation is interpreted as the minimum pressure of melt segregation, yet on the Moon these pressures translate to depths of 350 to more than 500 km.. The physics of transporting melt these distances through cracks without altering the melt composition have been modeled (4) and the possibility of such transport seems remote at a time in lunar history when the thickness of the elastic lithosphere was on the order of 50 to 100 km (5). Thus polybaric melting models analogous to those proposed for terrestrial midocean ridge basalts (6) provide attractive alternatives. Because of the paucity of data, algorithms in the polybaric melting model proposed by the author (1) depended upon several extraoplations of phase equilibria and crystal/liquid partitioning from experiments at lower pressures on terrestrial compositions, so a series of melting experiments was initiated to provide data at high pressure with which to test and refine the model.

Partially crystallized glasses were synthesized with compositions designed to produce multiply-saturated liquids at high pressure and run in high purity iron capsules for 1 to 2 days in a piston-cylinder apparatus. The resulting charges contained remarkably homogeneous olivine + pyroxene ± garnet set in fine intergowths of quench crystals. In one charge a comparison of the average of 36 spot analyses (electron microprobe) collected on a grid was compared with the average of 4 rastered-beam analyses (100 μm on a side): all elements agreed within the standard deviations indicating that raster analyses of highly mafic quench intergrowths (no plagioclase) are accurate. Fig. 1 shows the compositions of melts in equilibrium with ol and opx (open squares) together with segments of the ol + opx liquidus boundary calculated for each melt according to the algorithms in (1). In each case except at 25 kbar the melt composition has a slightly higher Qtz component than the predicted liquidus boundary, however, the differences are not significant with respect to the overall uncertainty of the model.

The new experiments also provide relevant data on partitioning and phase equilibria. There is a dramatic increase in the molar partition coefficient (D*) for Al_2O_3 between opx and liquid(liq) from an average value of ~0.1 at low pressure to a value of 0.5 at 30 to 40 kbar. Values of D* for TiO_2 and Cr_2O_3, however, remain constant (~0.15 and ~ 2, respectively) over this pressure range. The different behaviors can be explained in terms of liquid structure: Al is tetrahedrally coordinated in silicate liquids at low pressure, but these tetrahedral sites become increasingly unfavorable with respect to the octahedral sites available in pyroxene as pressure increases; whereas Ti and Cr find no greater advantage in pyroxene with increasing pressure because they are already in octahedral sites in the liquid at low pressure. The previous model (1) employed a single value of D* (0.35) for opx and liq at high pressure that is now obviously too low for pressures in the range of 30 to 40 kbar. A consequence of using a pressure-dependent D* for Al is that now it is more difficult to deplete the source in Al_2O_3 at high pressure and extraction of melt at each pressure must, therefore, be more efficient to produce a polybaric pooled melt with green glass composition.

Fig. 2 shows the approximate location of liquidus boundaries at 25 kbar (dashed curves) in two projections based on multiply-saturated experimental liquid compositions (squares). Crystal compositions are shown as circles. Phase equilibria at 30 kbar are similar albeit displaced slightly farther away from Qtz. It is not clear yet whether in these intermediate Mg' liquids there is a liquidus boundary in the {Ol} projection separating fields of ol + pigeonite(pig) and ol + aluminous augite(aug) or whether there is a single continuous field of ol + clinopyroxene (cpx). In any case because most estimates of lunar mantle compositions have low Wo contents, melting of the interior at P > 25 kbar probably begins in the presence of ol, opx, and pig. Similar behavior has been observed in experiments on martian analogs (7). If there is sufficient Al in the source to stabilize garnet(gar), as there is in most estimates of whole Moon composition (8), then the equilibrium at the solidus will be opx + liq = ol + gar + pig. As in the case of the martian analogs, the initial melt will be nepheline-normative.

Finally, the Fe-Mg exchange coefficient for ol and liq (K_D) has similar values in the high pressure experiments as in previously reported low pressure experiments on lunar basalts (3) at comparable concentrations of TiO_2 (cf. Fig. 3 in ref. 3). However, even though TiO_2 levels are similar, the silica contents of the high pressure liquids are much lower than those of the basalts, so that tendency for increasing pressure to

increase K_D at constant composition (9) is offset by the shift in the ol + opx liquidus boundary to lower silica with increasing pressure.

REFERENCES

(1) Longhi J. (1992) *Proc. Lunar Planet. Sci. 22, 343-353.* (2) Delano J.W. (1986) *J. Geophys. Res. 91,* D201-D213. (3) Longhi J. (1992) *Geochim. Cosmochim. Acta, 56,* 2235-2251. (4) Spera F. J. (1992) *Geochim. Cosmochim. Acta, 56,* 2253-2265. (5) Solomon S.C. and Head J.W. (1979) *J. Geophys. Res. 84,* 1667-1682. (6) Klein E.M. and Langmuir C.H. (1987) *J. Geophys. Res. 92,* 8089-8115. (7) Bertke C. M. and Holloway J. R. (1990) *Lunar Planet. Sci. XXI,* 73-74. (8) BVSP (1981) *Basaltic Volcanism on the Terrestrial Planets,* Pergamon. (9) Ulmer P. (1989) *Contrib. Mineral. Petrol., 101,* 261-273.

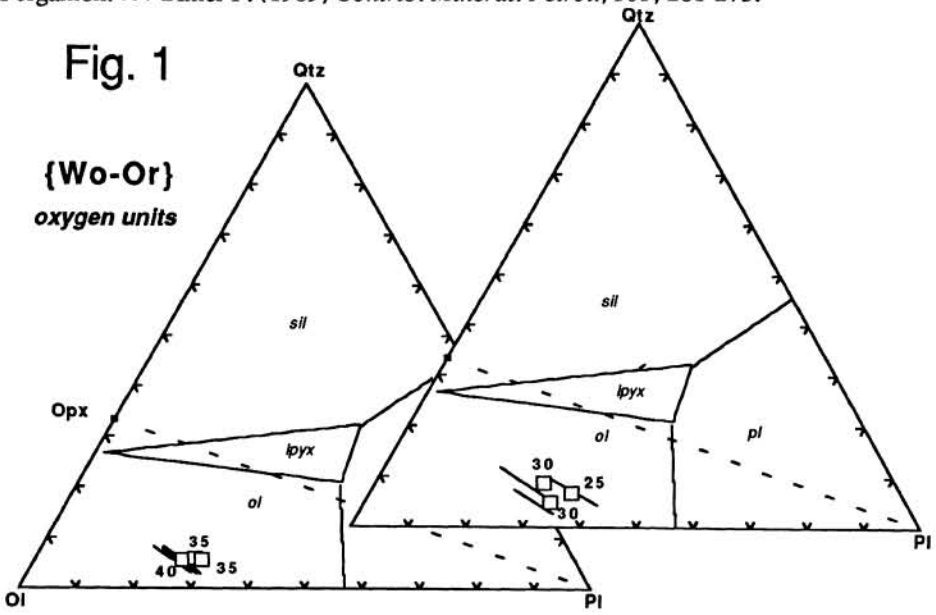

Fig.1. Comparison of positions of the ol + opx liquidus boundary in wollastonite (Wo) projection: squares are experimental determinations (this study); line segments are calculations of the liquidus boundary based on the algorithms of (1) and using the observed liquid compositions as inputs. Low pressure liquidus boundaries are shown for reference.

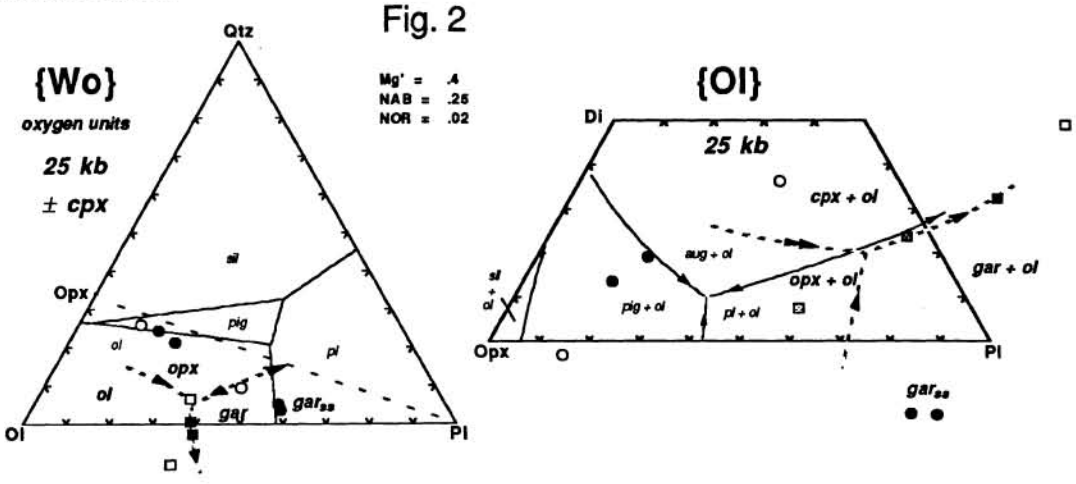

Fig. 2. Schematic liquidus equilbria at 25 kbar in Wo and Ol projections. ol-pig-gar-saturated liquids shown as solid squares; ol-opx- and ol-cpx-saturated liquids shown as open squares. Crystal compositions shown as solid or open circles as appropriate. Dashed curves are inferred 25 kbar liquidus boundaries; solid curves are 1 bar liquidus boundaries.